Supporting Information

An inorganic Co-containing heteropolyoxoniobate: reversible chemochromism and H_2O-dependent proton conductivity properties

Nian Shi, Yong-Jiang Wang, Xin-Xiong Li, Yan-Qiong Sun* and Shou-Tian Zheng*

College of Chemistry, Fuzhou University, Fuzhou, Fujian 350108, China.
*Email: sunyq@fzu.edu.cn; stzheng@fzu.edu.cn

Contents

1. Materials and Methods

All chemicals were commercially purchased and directly used without further purification except $K_7HNb_6O_{19}$•$13H_2O$ precursor was prepared as described in the literature.[1]

Preparation of aqueous solutions of Na_2CO_3/$NaHCO_3$ buffer solution (pH = 10.5):

Na_2CO_3 (5.96 g, 0.125 mol) and $NaHCO_3$ (0.84g, 0.01 mol) were added to 250.00 ml with deionized water with constant stirring to obtain Na_2CO_3/$NaHCO_3$ buffer solution (pH = 10.5).

$CoSO_4$ solution (0.5 mol•L^{-1}) was obtained by adding $CoSO_4$ •$7H_2O$ (2.81 g, 0.01 mol) to 10.00 ml deionized water with constant stirring.

Instruments: ICP analysis was conducted on an Ultima2 spectrometer.

Adsorption analysis: Water vapor adsorption tests were performed at 298K on a micromeritics 3flex Adsorption Analyzer. Sample **1** were activated by degassed under high vacuum at 313K for 12h to obtain the evacuated samples.

Proton conduction experiments:

Ac impedance measurements were carried out with a zennium/IM6 impedance analyzer over the frequency range from 0.1 Hz to 5 MHz with an applied voltage of 50mV. The relative humidity was controlled by a STIK Corp. CIHI-150B incubator. The sample was pressed to form a cylindrical pellet of crystalline powder sample (~1.6 mm thickness ×5 mm ϕ) coated with Cpressed electrodes. Two silver electrodes were attached to both sides of pellet to form four end S3 terminals (quasi-four-probe method). The bulk conductivity was estimated by semicircle fittings of Nyquist plots.

2. Tables

Table S1 ICP analyses of 1-purple. (The total amount of Si、Nb and Co is normalized to 100 %.)

Atom	Calculated (%)	Found (%)
Nb	95.0543	95.2987
Co	3.3496	3.1429
Si	1.5963	1.4742

Table S2. The bond valence sum calculations of the Si、Nb and Co atoms.[2]

Atom Code	Bond Valence	Valence state	Atom Code	Bond Valence	Valence state	Atom Code	Bond Valence	Valence State
Nb1	5.20023	5	O9	1.70730	2	O37	1.82246	2
Nb2	4.95066	5	O10	1.81168	2	O38	1.74154	2
Nb3	4.95231	5	O11	1.64789	2	O39	1.81968	2
Nb4	4.96248	5	O12	1.67753	2	O40	1.72745	2
Nb5	4.99310	5	O13	1.77290	2	O41	1.19426	1
Nb6	5.03317	5	O14	1.60035	2	O42	1.77200	2
Nb7	5.12565	5	O15	1.80408	2	O43	1.98317	2
Nb8	5.12127	5	O16	1.97397	2	O44	1.77967	2
Nb9	5.19242	5	O17	2.00903	2	O45	1.72915	2
Nb10	5.04447	5	O18	2.07151	2	O46	2.01853	2
Nb11	5.09846	5	O19	1.65911	2	O47	1.69909	2
Nb12	5.25008	5	O20	1.76774	2	O48	1.79547	2
Nb13	5.06687	5	O21	1.78763	2	O49	1.79643	2
Nb14	4.85862	5	O22	1.94308	2	O50	1.66099	2
Nb15	5.16563	5	O23	1.76403	2	O51	1.71568	2
Nb16	4.96462	5	O24	1.74308	2	O52	0.42165	0
Nb17	5.09786	5	O25	1.77978	2	O53	1.63329	2
Nb18	5.02011	5	O26	1.96890	2	O54	1.68319	2
Co1	2.07066	2	O27	1.83234	2	O55	1.62054	2
Si1	3.83542	4	O28	1.81243	2	O56	0.23155	0
O1	1.64487	2	O29	1.95795	2	O57	0.16038	0
O2	1.82773	2	O30	1.81375	2	O58	0.36359	0
O3	2.03162	2	O31	1.78751	2	O59	0.34725	0
O4	1.59584	2	O32	1.77557	2	O60	0.18352	0
O5	1.67299	2	O33	1.81228	2	O61	0.17737	0
O6	1.78981	2	O34	1.77374	2	O62	0.16964	0
O7	1.22591	1	O35	0.26777	0	O64	0.20546	0
O8	1.80100	2	O36	1.79209	2	O65	0.21225	0

Table S3 Crystal data and structure refinement parameters for compound 1-purple

Compound	**1-purple**
Empirical formula	$CoH_{63}KNa_2Nb_{18}O_{81}Si$
M_r (g·mol^{-1})	3203.83
Temperature (K)	175(2)
Crystal system	monoclinic
Space group	$P2_1/c$
a (Å)	13.0639(14)
b (Å)	18.0707(18)
c (Å)	35.154(4)
α (°)	90.00
β (°)	97.5842(19)
γ (°)	90.00
V / Å^3	8226.3(15)
Z	4
ρ_{calcd} (g/cm^3)	2.493
M (mm^{-1})	2.768
F(000)	5808
2θ range / °	3.24 to 50.12
R_{int}	0.0501
GooF	1.063
R_1 [I>2σ]	$R_1{}^a$ = 0.0775 $wR_2{}^b$ = 0.1779
R_1(all data)	$R_1{}^a$ = 0.0842 $wR_2{}^b$ = 0.1819

[a]R_1=∑||Fo|–|Fc||/∑|Fo|, [b]wR_2={∑[w(F$_o^2$–F$_c^2$)^2]/∑[w(F$_o^2$)^2]}$^{1/2}$.

Table S4 Crystal cell parameters of 1-purple and 1-blue

	1-purple 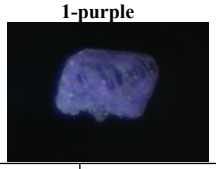	**1-blue** 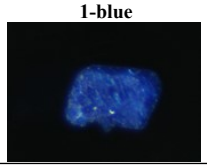
Crystal system	**monoclinic**	**monoclinic**
a/Å	**13.06**	**12.33**
b/Å	**18.07**	**17.53**
c/Å	**35.15**	**30.27**
α/°	**90**	**90**
β/°	**97.58**	**94.17**
γ/°	**90**	**90**
Volume/Å^3	**8226.3**	**6522**

As shown in Table S4 and Fig.S9, when the color of **1-purple** crystals gradually changed from purple to blue, the cell parameters became smaller. The crystal system remains monoclinic, but the volume of unit cell is reduced by 20.7%. The loss of water molecules resulted in the chromic behavior and the shrinking of unit cell. Unfortunately, because the crystal quality of **1-blue** is too poor, the detailed crystal structural data of **1-blue** cannot be obtained.

The *a*, *b* and *c* of **1-purple** were 13.06 Å, 18.07 Å and 35.15 Å, respectively and the volume was 8226.3 $Å^3$, while *a*, *b* and *c* of **1-blue** were 12.335 Å, 17.53 Å and 30.27 Å respectively and the volume was 6522 $Å^3$. The *a*, *b* and *c* were reduced by about 0.73 Å, 0.54 Å and 4.88 Å while the volume is reduced by about 1700 $Å^3$.

Table S5. The calculation of the proton conductivity and the activation energy (E_a) of 1-purple

T/K	R/Ω	σ/ S cm-1	lnσT	1000/T	Slope	Ea
298.15 (25°C)	1526.8	4.54E-04	-2.000321821	3.354016435		
308.15 (35°C)	1046.7	6.62E-04	-1.589800175	3.245172805		
318.15 (45°C)	770.19	9.00E-04	-1.251103484	3.14317146	-4.32544	0.36 eV
328.05 (55°C)	541.61	1.28E-03	-0.868369365	3.048315806		
338.15 (65°C)	288.59	2.40E-03	-0.208506627	2.957267485		
348.15 (75°C)	68.263	1.01E-02	1.262276314	2.872325147		

Table S6. The calculation of the proton conductivity for 1-blue at 70% RH and room temperature with the chromic response (purple to dark blue) by adsorbing the water vapour

	L/cm	S/cm^2	R/Ω	σ/ $S\ cm^{-1}$
Blue	**0.136**	**0.1963**	**108200**	**6.40E-06**
2min	**0.136**	**0.1963**	**96045**	**7.21E-06**
4min	**0.136**	**0.1963**	**84151**	**8.23E-06**
6min	**0.136**	**0.1963**	**73826**	**9.38E-06**
8min	**0.136**	**0.1963**	**73826**	**9.38E-06**
10min	**0.136**	**0.1963**	**58469**	**1.18E-05**
14min	**0.136**	**0.1963**	**47365**	**1.46E-05**
20min	**0.136**	**0.1963**	**37986**	**1.82E-05**
28min	**0.136**	**0.1963**	**28982**	**2.39E-05**
38min	**0.136**	**0.1963**	**20733**	**3.34E-05**
52min	**0.136**	**0.1963**	**14237**	**4.87E-05**
66min	**0.136**	**0.1963**	**9467.9**	**7.32E-05**
74min	**0.136**	**0.1963**	**4939.3**	**1.40E-04**
……	**……**	**……**	**……**	**……**
Pink	**0.136**	**0.1963**	**4595.7**	**1.51E-04**

Table S7 A summary of known vapor adsorption capacity of POMs materials

Compounds	*Amount(cm^3g^{-1})*	*ref.*
1	**169**	**This work**
$[Cu(en)_2]_6\{[Cu(en)_2]@\{[Cu_2(trz)_2(en)_2]_6[H_{10}Nb_{68}O_{188}]\}\}$	224	3
$H_{20}Cu(en)[Cu(en)_2]_{11}\{[Cu(en)_2]@\{[Cu_2(en)_2(trz)_2]_6(Nb_{68}O_{188})\}[4\text{-Tzp}]\}_{12}\cdot 22en\cdot 130H_2O$	219	4
$[MoV_{180}MoV_{160}(OH)_{60}O_{620}\text{-}x(SO_3)_{20}\text{-}x(SO_4)x]^{(80\text{-}2x)}\cdot guest$	212	5
$[Cu(en)_2(H_2O)]_2\{[Cu(en)]_4[Cu(en)_2]_5\{[Cu(en)_2KNb_{24}O_{72}H_{10}]_2\}\cdot 6en\cdot 70H_2O$	204	6
$K_4@\{[Cu_{29}(OH)_7(H_2O)_2(en)_8(trz)_{21}][Nb_{24}O_{67}(OH)_2(H_2O)_3]_4\}$	193	3
$[Cu(en)_2]@\{[Cu_2(en)_2(trz)_2]_6(Nb_{68}O_{188})\}$	188	3
$H_{12}\{[Cu(en)_2]_6[Nb_{68}O_{176}(OH)_{12}(H_2O)_{12}]\}_{52}H_2O$	172	7
$[Zn_{12}(trz)_{20}][SiW_{12}O_{40}]\cdot 11H_2O$	150	8
$K_3[Cr_3O(OOCH)_6(H_2O)_3][R\text{-}SiW_{12}O_{40}]$	130	9
$Cu_6(Trz)_{10}(H_2O)_4[H_2SiW_{12}O_{40}]\cdot 8H_2O$	118	10
$[Cu_4(dpdo)_{12}][H(H_2O)_{27}(CH_3CN)_{12}][PW_{12}O_{40}]_3$	65.1	11
$K_2[Cr_3O(OOCH)_6(mepy)_3]_2[\alpha\text{-}PMo_{12}O_{40}]\cdot 5H_2O$	56.8	12
$H_{14}[Na_6(H_2O)_{12}]_4[K_{42}Ge_8W_{72}O_{272}(H_2O)_{60}]\cdot solvent$	52	13
$[Cu_3(L)_2(H_2O)_4][Cu(dmf)_4(SiW_{12}O_{40})]\cdot 9H_2O$	51.7	14
$H[Ni(Hbpdc)(H_2O)_2]_2[PW_{12}O_{40}]\cdot 8H_2O\}$	31	15
$[Co(pn)_3]_4[PNb_{12}O_{40}(VO)_6][OH]_5\cdot 20H_2O$	19.72	16
$(DODA)_{23}[Mo_{154}O_{462}H_5]\cdot 70H_2O$	16.6	17
$Cs_{3.6}K_{0.4}[PW_{11}O_{39}(Sn\text{-}OH)]\cdot 8H_2O$	0.31	18
$K_2[Cr_3O(OOCH)_6(mepy)_3]_2[a\text{-}SiW_{12}O_{40}]\cdot 2H_2O\cdot CH_3OH$	0.03	19
$Cs_2[Cr_3O(OOCC_2H_5)_6(H_2O)_3]_2[R\text{-}SiW_{12}O_{40}]\cdot 4H_2O$	0.022	20,21
$Cs_3H_{0.3}[SiW_{12}O_{40}]_{0.83}\cdot 3H_2O$	0.020	22

[a] Trz: 1,2,4-triazole; dpdo: 4,4'-bipyridine-N,N'-dioxide; mepy: 4-methylpyridine; L: *N,N*-bis[(2-hydroxy-3-methoxyphenyl)methylidene] hydrazine hydrate; dmf: N,N-Dimethylformamide; H2bpdc : 2,2'-bipyridyl-3,3'-dicarboxylicacid ; pn: 1,2-diaminopropane ; DODA: dimethyldioctadecylammonium.

3. Additional data and figures

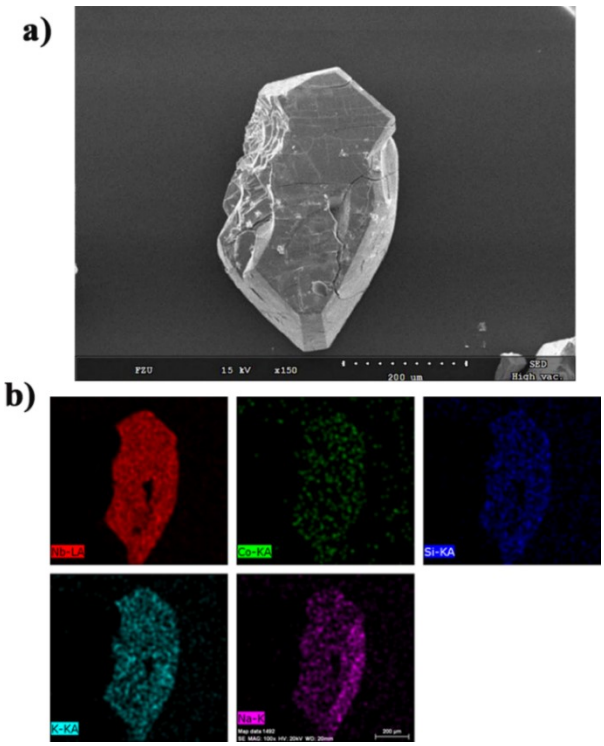

Fig. S1 Scanning electron microscope and EDS image compound **1-purple**

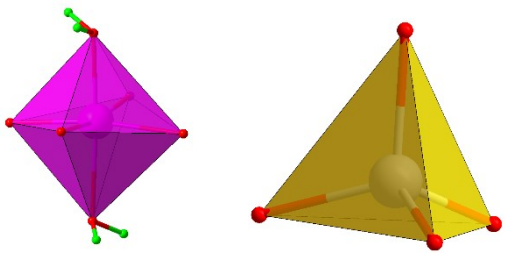

(a) (b)

Fig. S2 (a) View of the octahedron coordinated environment of Co(II) center; (b) View the tetrahedron coordinated environment of Si(IV) center.

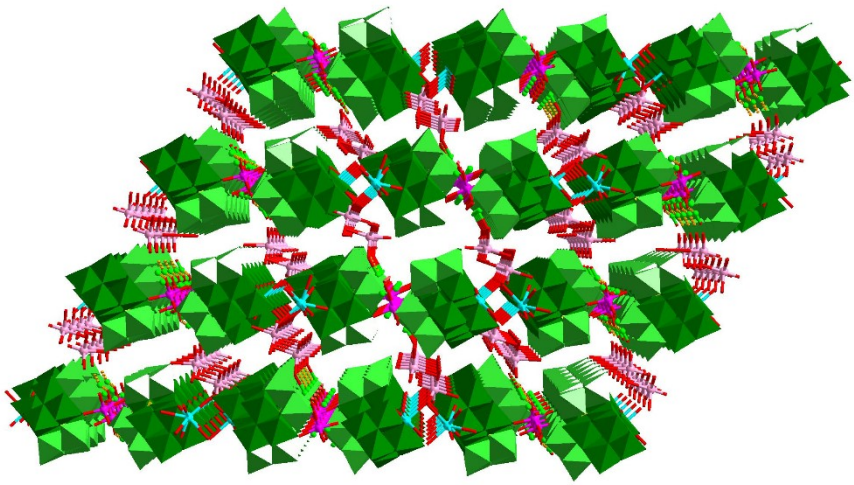

Fig. S3 View of the three-dimensional supramolecular structure of **1-purple**. Atomic color code: Co, purple; O, red; H, green; K, cyan; Na, pink. Polyhedral color codes: NbO_6, green; SiO_4, yellow.

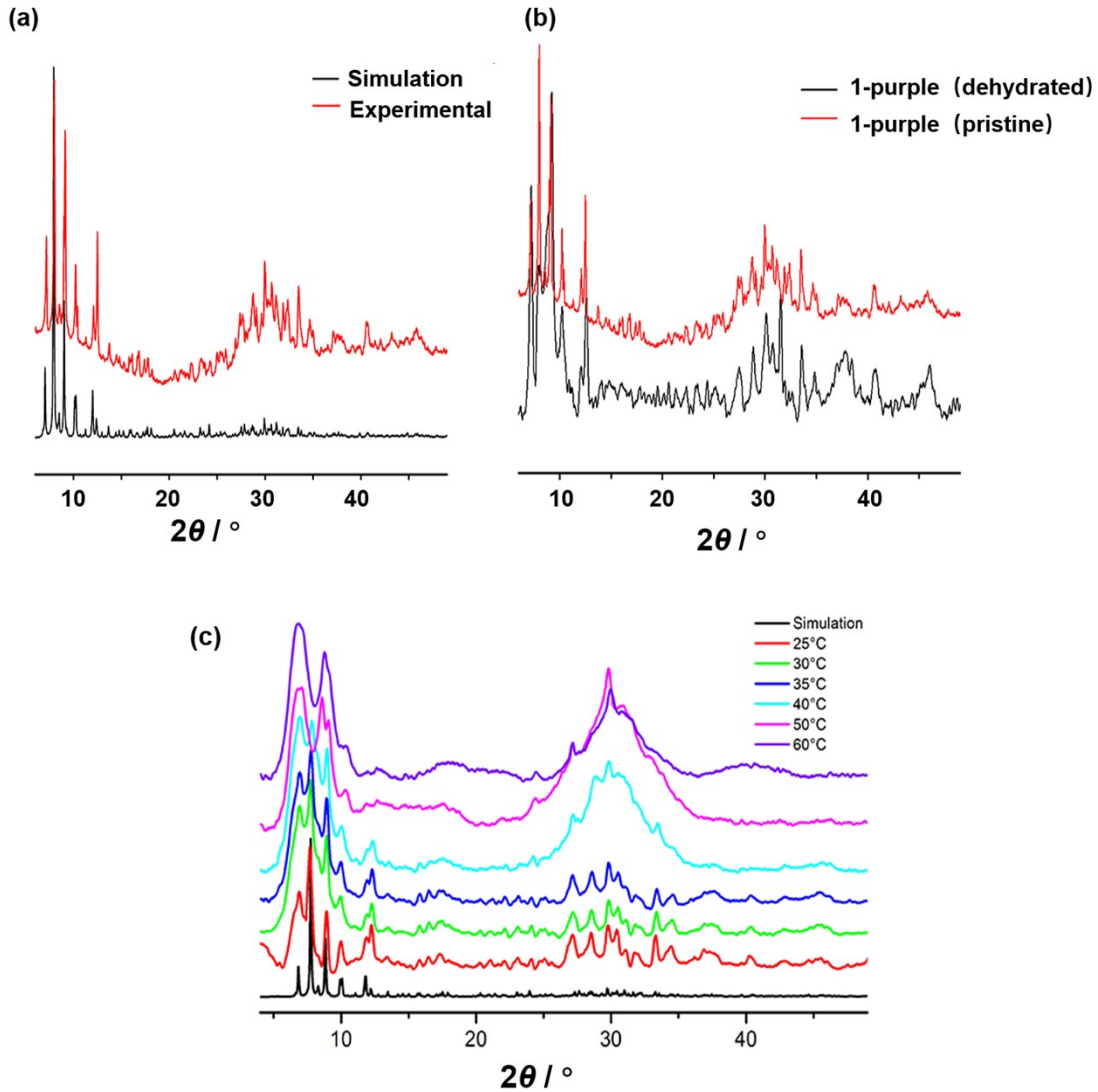

Fig. S4 (a) Simulated and experimental PXRD patterns of **1-purple**; (b) PXRD patterns of the compound **1-purple** (pristine) and **1-purple** (dehydrated); (c) The PXRD patterns of the compound **1-purple** at different temperatures.

The phase purity of compound **1-purple** was confirmed by powder X-ray diffraction (PXRD) measurement (Fig. S4a). The result shows that the experimental peaks matched well with the simulated values, indicating that there are no impurities in the sample, and PXRD patterns at different temperatures testify that the crystallinity of **1-purple** remains intact up to 40°C (Fig. S4c). The completely dehydrate dark blue sample of compound **1-blue** can uptake the water in vapor or liquid forms to recover the original purple color with revival of starting crystalline framework (Fig S4b).

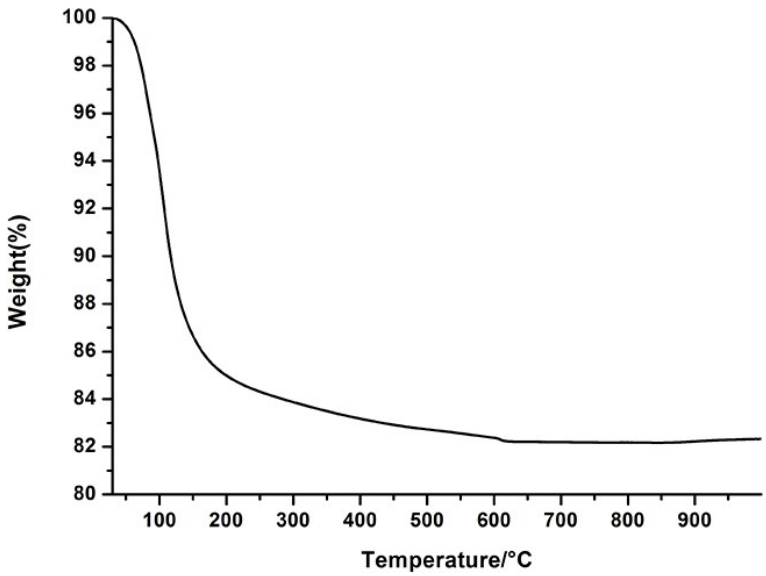

Fig. S5. TG curve of compound **1.**

Thermal gravimetric analysis (TGA) of **1** was performed under nitrogen atmosphere in the range 25–1000 °C. Thermogravimetric analysis exhibits that the first continuous weight loss ratio from room temperature to 200 ℃ is 15.01%, which may be ascribed to the loss of coordinated and free water molecules, and its theoretical weight loss ratio is 15.17%(Fig. S5).

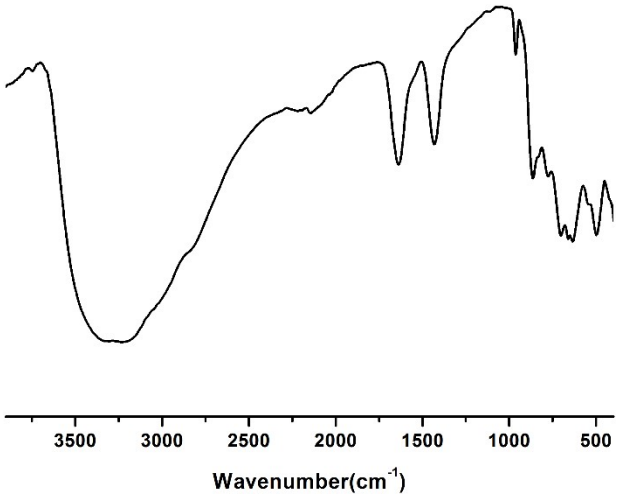

Fig. S6 IR spectrum of the compound **1-purple**

The IR spectrum of **1-purple** shows that the wide peak around 3320 cm $^{-1}$ can be attributed to the stretching vibration of the O-H group of the water and the O H of the coordinated hydroxyl group. The peak at 1623 cm $^{-1}$ corresponds to the H O H bending vibration of crystal water. The characteristic stretching vibration peak of Si O is at 970 cm^{-1}. The peaks in the range of 600 - 1000 cm $^{-1}$ may be attributed to ν_{as} (Nb O$_c$ Nb) , ν_{as} (Nb–O$_b$ Nb), ν_{as} (Nb O$_t$) stretching vibration peak. Co−O stretching vibration is at 472 cm^{-1}, which is consistent with the results of X-ray single crystal diffraction of **1-purple**.

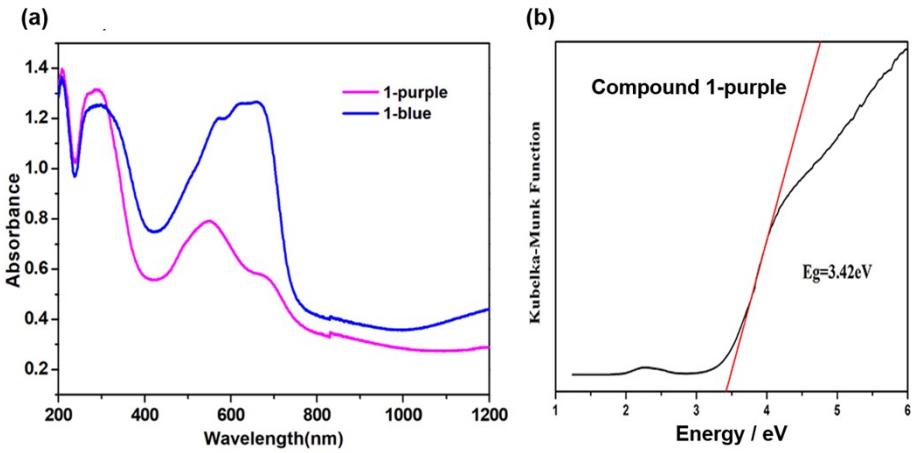

Fig. S7 (a) The solid UV-vis absorption spectra for **1-purple** (pristine) and **1-blue** (dehydrated); (b) The solid UV diffuse spectrum of compound **1.**

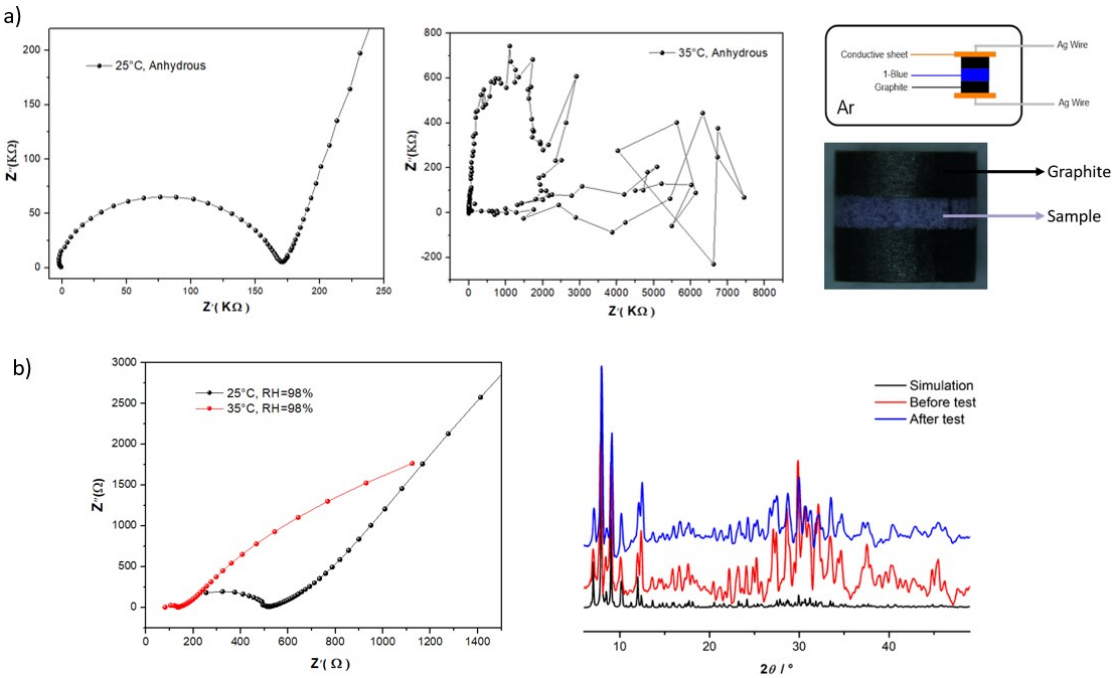

Fig. S8 a) Nyquist plots for 1-blue at different temperature conditions under anhydrous conditions and Device diagram. b) Nyquist plots for 1-purple at different temperature conditions with 98% RH and the powder diagram before and after the test.

Fig. S8a showed that the impedance value of dehydrated **1-blue** is very large, and the corresponding proton conductivity is 6.34×10^{-6} S cm^{-1} under anhydrous condition at 25°C. When the temperature raised to 35°C, the measured impedance data became irregular. According to the crystal structure of **1-purple**, The completely dehydrate dark blue sample of compound **1-blue** can be ascribed to the tetra-coordinated geometry of Co(II) center owing to the removal of coordinated water molecules. When the temperature raised, the hydrogen bonds may completely destroy inside the crystal, so the proton conductivity became small and irregular above 35°C and there are no enough proton conductivity data at different temperature to fit Arrhenius plots. We are very sorry that the Arrhenius plots can't be obtained under anhydrous condition.

Fig. S8b shows that the proton conductivity of **1-purple** increases from 6.71×10^{-4} S cm^{-1} to 2.55×10^{-3} S cm^{-1} at RH = 98% when the temperature raises from 25 to 35°C. The PXRD patterns before and after impedance measurements confirm that the crystals keep stable to 35°C under higher RH condition. When the temperature is above 35°C, the crystal structure would collapse at RH = 98%, and it impossible to continue the proton conductivity test. So the crystal cannot keep stable under high temperature and high humidity.

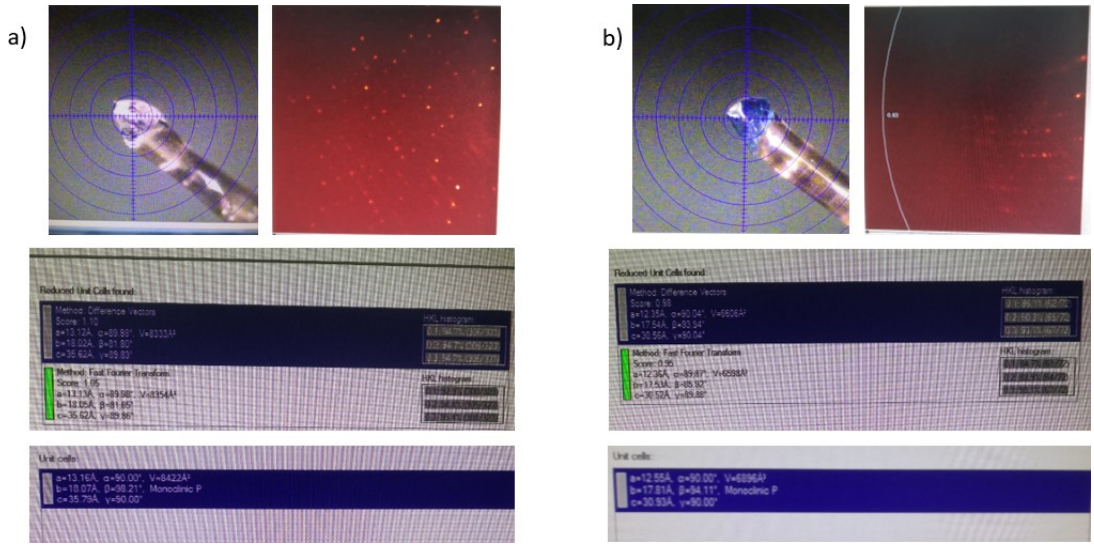

Fig. S9 a) Crystal photos and crystal data of 1-purple; b) Crystal photos and crystal data of 1-blue.

Notes and references

1. M. Filowitz, R. K. C. Ho, W. G. Klemperer and W. Shum, *Inorganic Chemistry*, 1979, **18**, 93 -103.
2. I. D. Brown, D. Altermatt, *Acta Crystallogr. Sect. B: Struct. Sci*, 1985, **41**, 244−247.
3. Z.-K. Zhu, Y.-Y. Lin, H. Yu, X.-X. Li, S.-T. Zheng, Angew. Chem. Int. Ed., 2019, 58, 16864.
4. Z.-K. Zhu, Y.-Y. Lin, L.D.-Lin, X.-X. Li, Y.-Q. Sun and S.-T. Zheng, Inorg. Chem., 2020, 59, 11925.
5. J.-M Lin, N. Li, S.-P. Yang, M.-J. Jia, J. Liu, X.-M. Li, L. An, Q.-W. Tian, L.-Z. Dong, Y.-Q. Lan, J. Am. Chem. Soc., 2020, 142, 13982.
6. Z.-K. Zhu, L.-D. Lin, J. Zhang, X.-X. Li, Y.-Q. Sun and S.-T. Zheng, Inorg. Chem. Front., 2020, 7, 3919.
7. Y.-D. Lin, Z.-K. Zhu, R. Ge, H. Yu, Z. Li, C. Sun, Y.-Q. Sun, X.-X. Li and S.-T. Zheng, Chem. Commun., 2021,57, 4702
8. E.-L. Zhou, C.-Qin, X.-L. Wang, K.-Z. Shao and Z.-M. Su, Chem. Eur. J., 2015, 21, 13058.
9. S. Uchida, R. Kawamoto, N. Mizuno, Inorg. Chem., 2006, 45, 5136.
10. E.-L. Zhou, C. Qin, P. Huang, X.-L. Wang, W.-C. Chen, K.-Z. Shao and Z.-M. Su, Chem. Eur. J., 2015, 21, 11894.
11. M. Wei, L. Chen, X. Duan, J. Coord. Chem., 2014, 67, 2809.
12. R. Kawahara, S. Uchida, N. Mizuno, Chem. Mater., 2015, 27, 2092.
13. Z. Li, L.-D. Lin, H. Yu, X.-X. Li and S.-T. Zheng, Angew. Chem. Int. Ed., 2018, 57, 15777.
14. M.-L. Wei.; J.-J. Sun, X.-Y. Duan, Eur. J. Inorg. Chem., 2014, 345.
15. M.-L. Wei, X.-X. Wang, J.-J. Sun and X.-Y. Duan, J. Solid. State. Chem., 2013, 202, 200.
16. J.-F. Hu, Y.-Q. Xu, D.-K. Zhang, B.-K. Chen, Z.-G. Lin and C.-W. Hu, Inorg. Chem., 2017, 56, 10844.
17. S. Noro, R. Tsunashima, Y. Kamiya, K. Uemura, H. Kita, L. Cronin, T. Akutagawa, T. Nakamura, Angew. Chem. Int. Ed., 2009, 48, 8703.
18. Y. K. Miura, H. Imai, T. Yokoi, T. Tastumi, Y. Kamiya, Microporous Mesoporous Mater., 2013, 174, 34.
19. S. Uchida, R. Eguchi, N. Mizuno, Angew. Chem. Int. Ed., 2010, 49, 9930.
20. A. Lesbani, R. Kawamoto, S. Uchida, N. Mizuno, Inorg. Chem., 2008, 47, 3349.
21. C. J. Jiang, A. Lesbani, R. Kawamoto, S. Uchida, N. Mizuno, J. Am. Chem. Soc., 2006, 128, 14240.
22. Y. Ogasawara, S. Uchida, T. Maruichi, R. Ishikawa, N. Shibata, Y. Ikuhara, N. Mizuno, Chem. Mater., 2013, 25, 905.